JBIC Journal of Biological Inorganic Chemistry (2019) 24:419–432
https://doi.org/10.1007/s00775-019-01657-2

ORIGINAL PAPER

Synthesis and evaluation of the antileishmanial activity of silver compounds containing imidazolidine-2-thione

Patrícia Ferreira Espuri[1,5] · Larissa Luiza dos Reis[1] · Eduardo de Figueiredo Peloso[2] · Vanessa Silva Gontijo[3] · Fábio Antônio Colombo[1] · Juliana Barbosa Nunes[1] · Carine Ervolino de Oliveira[1] · Eduardo T. De Almeida[3] · Débora E. S. Silva[4] · Jessica Bortoletto[4] · Daniel Fonseca Segura[4] · Adelino V. G. Netto[4] · Marcos José Marques[1,5]

Received: 3 January 2019 / Accepted: 27 March 2019 / Published online: 4 April 2019

Abstract

A new series of silver compounds could be of interest on designing new drugs for the treatment of leishmaniasis. The compounds [Ag(phen)(imzt)]NO_3 ***(1)***, [Ag(phen)(imzt)]CF_3SO_3 ***(2)***, [Ag(phen)$_2$](BF_4)·H_2O ***(3)***, [Ag_2(imzt)$_6$](NO_3)$_2$ ***(4)***, and ***imzt*** have been synthesized and evaluated in vitro for antileishmanial activity against *Leishmania.* (*L.*) *amazonensis* (La) and *L.* (*L.*) *chagasi* (Lc), and two of them were selected for in vivo studies. In addition to investigating the action on *Leishmania*, their effects on the hydrogen peroxide production and cysteine protease inhibition have also been investigated. As for antileishmanial activity, compound ***(4)*** was the most potent against promastigote and amastigote forms of La (IC_{50} = 4.67 and 1.88 μM, respectively) and Lc (IC_{50} = 9.35 and 8.05 μM, respectively); and comparable to that of amphotericin B, reference drug. Beside showing excellent activity, it also showed a low toxicity. In the in vivo context, compound ***(4)*** reduced the number of amastigotes in the liver and spleen when compared to the untreated group. In evaluating the effect of the compounds on *Leishmania*, the level of hydrogen peroxide production was maintained between the lag and log phases; however, in the treatment with compound ***(4)*** it was possible to observe a reduction of 25.44 and 49.13%, respectively, in the hydrogen peroxide rates when compared to the lag and log phases. It was noticed that the presence of a nitrate ion and ***imzt*** in compound ***(4)*** was important for the modulation of the antileishmanial activity. Thus, this compound can represent a potentially new drug for the treatment of leishmaniasis.

Electronic supplementary material The online version of this article (https://doi.org/10.1007/s00775-019-01657-2) contains supplementary material, which is available to authorized users.

Extended author information available on the last page of the article

Graphical abstract

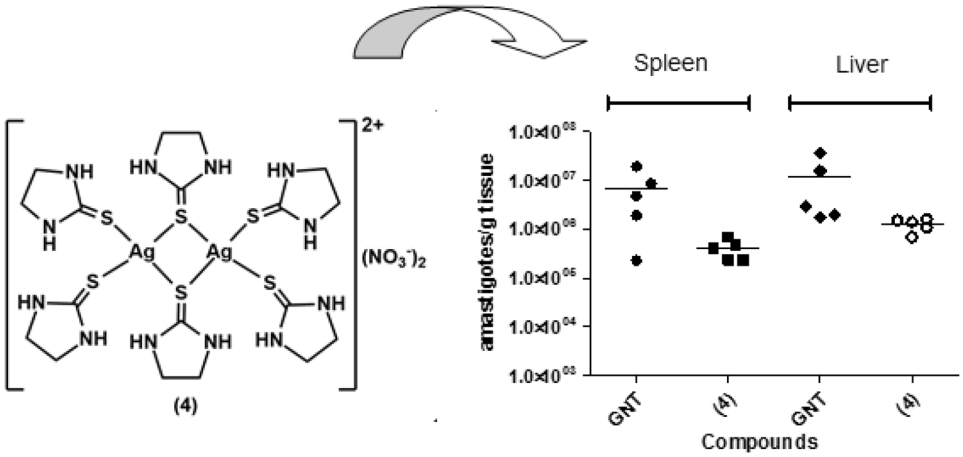

Keywords *Leishmania* · Silver compounds · Biological effects

Introduction

Leishmaniasis is a chronic intracellular infectious disease caused by the protozoan parasite of the genus *Leishmania* through the bite of infected phlebotomine sand fly [1, 2]. The disease is endemic in large areas of the tropics, subtropics and Mediterranean basin, spanning more than 98 countries [3]. About 350 million people are susceptible to the disease [4], which is classified as one of the most important neglected tropical diseases [5]. *Leishmania* parasites produce a broad spectrum of clinical manifestations in humans and other mammals, ranging from asymptomatic infection to fatal disease [6], including visceral, cutaneous and mucocutaneous symptoms, depending on complex interactions between the parasite and host's immune response [7].

Leishmaniases are diseases that have been neglected by the pharmaceutical industry. There is no human vaccine; and the drugs available are limited because of the high cost, toxicity, side effects and increasing signs of resistance [4, 8–10]. The development of new, inexpensive and safe drugs for the treatment of leishmaniasis remains a great challenge for researchers worldwide [11, 12].

Parallel, silver nanoparticles belong to the category of strong antimicrobial agents [13] and act as a growth promoter [14] as well as an immune booster [15] at limited doses, and hence, are used for treating wounds and burns [16]. Studies show that internalized Ag nanoparticles in human cells can be translocated to target organelles to elicit several biological effects, including alterations in cellular morphology, oxidative stress, DNA damage, inflammation, genotoxicity and mitochondrial alterations dysfunction, with subsequent apoptotic or necrotic cell death [17, 18]. It was also reported that silver nanoparticles used as an antibacterial agent appeared to provide protection against the bacterial challenge [19].

Beside the interest in silver nanoparticles, the potential medical applications of silver complexes have become an active and exciting research field in biological and bioinorganic chemistry [20]. Antibacterial activity of silver complexes depends on their stability and solubility in aqueous solution, lipophilicity and rate of release of the Ag^+ ions [20]; therefore, a careful choice of appropriate ligands is of crucial importance. Among the available ligands to provide new active silver-containing compounds, 1,10-phenanthroline (phen) and its derivatives are a good choice because they have the ability to act on a wide variety of biological processes [21]. In particular, silver complexes incorporating phenanthroline-type ligands have been found to be extremely active in vitro against several pathogens, including *Leishmania*. For instance, silver compounds of the type $[AgL_2]NO_3$ (L = polypyridyl ligands) also were shown to be biologically active against *Leishmania mexicana*, through interaction with DNA [22]. In our previous report, we have described the synthesis of ternary compounds of the type $[\{Ag(phen)(\mu\text{-tu})\}_2]X_2$ ($X = NO_3$; CF_3SO_3), where tu = thiourea), which were demonstrated to be effective in vitro against promastigote and intracellular amastigotes forms of *Leishmania* (*L.*) *amazonensis* and less toxic to murine peritoneal macrophages [23]. The discovery of the antileishmanial activity of such silver-containing compounds with low toxicity has motivated us to investigate their potential uses in antileishmanial chemotherapy. Thus, we have initiated a research program aiming to identify those parts of the molecular structure

that are important to the antileishmanial activity of these types of silver compounds. In this work, we hypothesized that the replacement of thiourea by imidazolidine-2-thione (imzt) would result in more active silver compounds, since imidazolidine-2-thiones are well-known to exhibit a wide range of biological activity [24].

In the current work, the compounds [Ag(phen)(imzt)]NO_3 ***(1)***, [Ag(phen)(imzt)]CF_3SO_3 ***(2)***, [Ag(phen)$_2$]$(BF_4)\cdot H_2O$ ***(3)*** {phen = 1,10-phenanthroline; imzt = imidazolidine-2-thione} and $[Ag_2(imzt)_6](NO_3)_2$ ***(4)*** have been synthesized and characterized by elemental analysis, infrared (IR), ^{1}H and ^{13}C NMR spectroscopies, MS/ESI and conductivity measurements. These silver-based compounds were tested against promastigote and amastigote forms of *L.* (*L.*) *amazonensis* and *L.* (*L.*) *infantum chagasi,* and their cytotoxicity against murine peritoneal macrophages in vitro was determined. In addition, the most promising compounds have been selected for further in vivo evaluation and their effects on *Leishmania* have denoted a possible mechanism of action.

Materials and methods

The compounds

The silver salts (Aldrich), 1,10-phenanthroline monohydrate (Aldrich) and imidazolidine-2-thione (Sigma) were employed without further purification. Acetonitrile (Merck) and chloroform (Tedia) of analytical purity were used as solvents. Deuterated dimethylsulphoxide (Sigma-Aldrich) solution was used for dissolution of the compounds of silver for NMR studies.

C, H, and N analyses were performed on a Leco Instruments LTDA—TruSpec CHNS (Federal University of Alfenas—UNIFAL-MG). Silver crucibles were used with the reference compounds EDTA, cysteine and acetaldehyde, according to the proposed carbon content. Conductivities of the complexes in DMSO solutions ($c = 1.0\times10^{-3}$ M) were determined on a Digimed-DM-31 conductometer. Electrospray mass spectrometric analyses were performed on a LCP Fleet—Thermo Scientific electrospray, operating in positive and negative-ion modes (sheath gas flow N_2: 8 a.u.; capillary voltage: in positive ion mode 20 V; ion transfer capillary temperature: 250 °C). Sample solutions (0.1 mg cm^{-3} in CH_3OH) were directly injected into the ESI source by use of a syringe pump at a flow rate of 20 mL min^{-1}. Infrared spectra were recorded as KBr pellets on a Spectrum 2000 Perkin Elmer spectrophotometer in the spectral range 4000–400 cm^{-1} with resolution of 2 cm^{-1}. ^{1}H and ^{13}C NMR spectra were obtained as *dmso*-d_6 solutions, on a Varian INOVA 500 spectrometer.

Synthesis

Compound [Ag(phen)(imzt)](NO_3) (1)

1,10-Phenanthroline monohydrate (0.37 mmol; 73.3 mg) dissolved in 10 mL of CH_3CN was added to a 10 mL CH_3CN solution containing $AgNO_3$ (0.37 mmol; 63.5 mg) leading to a yellow suspension. After stirring for 10 min, imidazolidine-2-thione (0.37 mmol; 38.2 mg) dissolved in 10 mL of CH_3CN was added. After stirring for 15 min, the product was isolated by simple filtration, washed with cold chloroform and dried under vacuum. Yield 30%. Anal. Calcd. for $C_{15}H_{14}AgN_5O_3S$ (%): C: 39.84; H: 3.12; N: 15.49. Found (%): C: 39.76; H: 3.10; N: 15.43. $\Lambda_M = 30\ \Omega^{-1}\ cm^2\ mol^{-1}$. FT-IR (KBr): 3161 ($\nu$NH), 2895 ($\nu_{as}CH_2$), 1533 ($\nu$CN + δNH), 1512 (ν_{ring}), 1320 (ν_sNO_2), 1094 (δCH), 823 (δNO_2), 722 (γCH), 494 cm^{-1} (νCS). ^{1}H NMR (ppm; t, triplet; d, doublet; s, singlet): 9.09 (dd, 4.4 Hz, 1.5 Hz, [2H], H1/H1′), 9.05 (s, 2H, NH), 8.71 (dd, 8.3 Hz, 1.4 Hz, [2H], H3/H3′), 8.14 (s, [2H], H4/H4′), 7.97 (m, [2H]. H2/H2′), 3.72 (s, [4H], –CH_2–). ^{13}C {^{1}H} NMR (ppm): 178.56 (C=S), 125.39–151.75 (C_{ar}), 45.31 (–CH_2–).

Compound [Ag(phen)(imzt)](CF_3SO_3) (2)

1,10-Phenanthroline monohydrate (0.39 mmol; 77.3 mg) dissolved in 10 mL of CH_3CN was added to a 10 mL CH_3CN solution containing $AgCF_3SO_3$ (0.45 mmol; 116.5 mg) affording a white suspension. After stirring for 10 min, imidazolidine-2-thione (0.41 mmol; 42 mg) dissolved in 10 mL of CH_3CN was added. After stirring for 15 min, the product was isolated by simple filtration, washed with cold methanol and dried under vacuum. Yield 76%. Anal. Calcd. for $C_{16}H_{14}AgF_3N_4O_3S_2$ (%): C: 35.63; H: 2.62; N: 10.39. Found (%): C: 35.7; H: 2.6; N: 10.2. $\Lambda_M = 45.3\ \Omega^{-1}\ cm^2\ mol^{-1}$. FT-IR (KBr): 3258 ($\nu$NH), 2895 ($\nu_{as}CH_2$), 1533 ($\nu$CN + δNH), 1513 (ν_{ring}), 1246 (νSO_3), 1224 (νCF_3), 1094 (δCH), 1027 (νSO_3), 723 (γCH), 498 cm^{-1} (νCS). ^{1}H NMR (ppm): 9.14 (dd, 4.4 Hz, 1.6 Hz, [2H], H1/H1′), 9.00 (s, 2H, NH), 8.76 (dd, 8.3 Hz, 1.6 Hz, [2H], H3/H3′), 8.18 (s, [2H], H4/H4′), 8.02 (m, [2H]. H2/H2′), 3.72 (s, [4H], –CH_2–). ^{13}C {^{1}H} NMR (ppm): 179.05 (C=S), 125.44–151.85 (C_{ar}), 45.28 (–CH_2–).

Compound [Ag(phen)$_2$](BF_4) H_2O(3)

1,10-Phenanthroline monohydrate (0.78 mmol; 140.6 mg) dissolved in 10 mL of CH_3CN was added to a 10 mL CH_3CN solution containing $AgBF_4$ (0.39 mmol; 76 mg) leading to a yellow suspension. After stirring for 15 min, the product was isolated by simple filtration, washed with cold methanol and dried under vacuum. Yield 70%. Anal. Calcd. for $C_{24}H_{18}AgBF_4N_4O$ (%): C: 50.3; H: 2.9;

N: 10.1. Found (%): C: 52.1; H: 3.0; N: 10.2. $\Lambda_M = 36.1$ Ω^{-1} cm^2 mol^{-1}. FT-IR (KBr): 3393 (νOH), 1510 (ν_{ring}), 1246 (νSO_3), 1224 (νCF_3), 1056 (νBF), 1027 (νSO_3), 725 (γCH), 522 (νBF). ^{1}H NMR (ppm): 9.14 (dd, 4.5 Hz, 1.5 Hz, [4H], H1/H1′), 8.76 (dd, 8.1 Hz, 1.4 Hz, [4H], H3/H3′), 8.20 (s, [4H], H4/H4′), 8.00 (dd, 8.1 Hz, 1.6 Hz, [4H]. H2/H2′).

Compound $[Ag_2(imzt)_6](NO_3)_2$ (4)

Complex $[Ag_2(imzt)_6](NO_3)_2$ ***(4)*** was synthesized as previously described [25]. Briefly, a hot solution of $AgNO_3$ (170 mg, 1 mmol) in water (2.5 mL) was added to a hot solution of imidazolidine-2-thione (315 mg, 3 mmol) in water (2.5 mL). Colourless crystals of the product were isolated upon cooling.

Biological assays

Determination of the proliferation curve

Promastigotes (10^6 mL^{-1}) were added to 25 cm^2 flasks containing LIT medium and were kept at 26 °C. On a daily basis, an aliquot was removed, and the number of promastigotes was determined using a Neubauer chamber [26, 27]. The experiments were carried out in triplicate and were repeated independently three times.

Antileishmanial activity against promastigotes

Promastigotes of *L.* (*L.*) *amazonensis* (strain MHOM/BR/71973/M2269) and *L.* (*L.*) *infantum chagasi* (strain MHOM/BR/1972/BH46) were grown on 24-well plates in LIT medium, supplemented with 10.0% (v/v) heat-inactivated foetal bovine serum and 1.0% penicillin (10,000 UI mL^{-1})/streptomycin (10.0 mg mL^{-1}) (Sigma, USA). Cells were harvested in the log phase, suspended in fresh medium, counted in Neubauer chambers and adjusted to a concentration of 1×10^6 cells mL^{-1}, using 24-wells plates. The compounds ***(1)***, ***(2)***, ***(3)***, ***(4)*** and ***Imzt*** were added to promastigote cultures (1×10^6 cells mL^{-1}) in the range of 0.10–40.00 µg mL^{-1}, solubilized in dimethyl sulfoxide (DMSO) (0.6%, v/v in all wells) and incubated at 25 °C. After 72 h of incubation, the surviving parasites were counted in a Neubauer's chamber and compared with controls, with just DMSO in concentration of 0.6% v/v, for the determination of 50.0% inhibitory growth concentration (IC_{50}). All tests were performed in triplicate at three different times and amphotericin B (Sigma) was used as the reference drug.

Antileishmanial activity against amastigotes

Murine peritoneal macrophages were maintained in RPMI 1640 medium (Sigma, USA) supplemented with 10.0% heat-inactivated foetal bovine serum at 37 °C in 5.0% CO_2 incubator. These cells were obtained from the peritoneal lavage of Swiss mice, properly approved by the Research Ethics Commission of the Universidade Federal de Alfenas (project number 08/2016) and were performed according to the Guide for the Care and Use of Laboratory Animals [11]. Cells were cultured in 24-well plates chamber on the glass slides of 13 mm (Nunc, USA) in a 8×10^5 cells density per well and infected with late log-phase promastigotes at a ratio of 10:1 (parasite/macrophage) and incubated at 37 °C in 5.0% CO_2 incubator for 24 h. Non-phagocytosed promastigotes were removed by washing, and compounds ***(1)***, ***(2)***, ***(3)***, ***(4)*** and ***Imzt*** solubilized in DMSO (from 0.10 to 40.00 µg mL^{-1}) were administered at the concentration of 0.6% v/v. After 72 h, chamber slides were fixed in absolute methanol, stained with 10.0% Giemsa and examined on an Optical Light Microscope in oil immersion. The percentage of infected cells per well was calculated taking account at least 200 macrophages. The ratio of inhibition (IC_{50} value) was calculated in comparative to the control only with DMSO. All assays were performed in triplicate at three different times using amphotericin B (Sigma) as the reference drugs.

Cytotoxicity evaluation

Murine peritoneal macrophages were obtained from the peritoneal lavage of Swiss mice, properly approved by the Research Ethics Commission of the Universidade Federal de Alfenas (project number 08/2016) and were performed according to the Guide for the Care and Use of Laboratory Animals [11]. A suspension of 8×10^5 murine peritoneal macrophages, in RPMI 1640 medium, supplemented with 10.0% heat-inactivated foetal bovine serum and 1.0% penicillin (10,000 UI mL^{-1})/streptomycin (10 mg mL^{-1}) were added to each well in 96-well plates. The plates were incubated in a 5.0% CO_2 air mixture at 37 °C to allow for adhesion of the cells. After 24 h, non-adherent cells were removed by washing with the RPMI 1640 medium. Then, several concentrations of compounds and reference drugs, ranging from 3.91 to 500.00 µg mL^{-1} in DMSO at the final concentration of 0.6% (v/v), were added to the wells containing the cells and the plates were incubated for more 48 h. Non-adherent cells were removed by washing with the RPMI 1640 medium. Afterwards, the 3-(4,5-dimethylthiazol-2-yl)-2,5-diphenyltetrazoliumbromide (MTT) was solubilized in PBS (5.0 µg mL^{-1}) as solvent, and 10 µL was added to RPMI 1640 medium in a final volume of 200.0 µL per well and incubated for 4 h [28]. Then, the medium was removed and

100.0 µL of DMSO was added to each well and homogenized for 15 min. Next, the absorbance of each individual well was calculated at 570 nm according to the following formula (OD represents optical density) using Eq. (1):

$$\text{Inhibition} = \left(\frac{\text{OD}_{\text{control}} - \text{OD}_{\text{compounds}}}{\text{OD}_{\text{control}} \times 100} \right). \quad (1)$$

Each experiment was performed in triplicate on three different occasions, and the percentage of viable cells was calculated taking into account the cell culture control (medium + cells + DMSO 0.6% v/v). The 50.0% cytotoxicity concentrations (CC_{50}) were determined and the selectivity index (SI) was established by the ratio between the values of CC_{50} and IC_{50} for amastigote forms.

Statistical analysis

The antileishmanial activities of the compounds were expressed as the concentration that inhibits the growth of 50.0% of the protozoan form (promastigote or amastigote). Statistical analysis was performed using non-linear regression to obtain the IC_{50} and CC_{50} values (cytotoxic concentration to 50.0% of the macrophages), followed by Tukey test and variance analysis. Differences of IC_{50} and/or CC_{50} between standard drug and compounds in question were significant when the p value was less than 0.05.

In vivo assay

Parasites and animals

L. (*L.*) *infantum chagasi* (strain MHOM/BR/1972/BH46) promastigotes were maintained in M-199 medium supplemented with 10% calf serum and 0.25% hemin, at 24 °C. Amastigotes were maintained by passaging in female golden hamsters (*Mesocricetus auratus*). Animals were kept in sterile absorbent material boxes, with food and water ad libitum, and in a natural light/dark cycle. All experimental procedures involving animals were approved by the Research Ethics Commission of the Universidade Federal de Alfenas (project number 08/2016) and were performed according to the Guide for the Care and Use of Laboratory Animals. For experimental infections, the spleens of infected animals were removed and macerated using a tissue grinder and the number of amastigotes was determined as described previously.

In vivo testing of experimental compounds against *Leishmania*

Female golden hamsters that had been recently weaned (120 g) were infected intraperitoneally with 1×10^7 amastigotes of *L.* (*L.*) *infantum chagasi* (MHOM/BR/1972/BH46) [29] and maintained in sterile absorbent material boxes, with water and food ad libitum. In the chronic phase (around 50 days of infection), animals were divided into four groups ($n = 5$/group), and subjected for 10 consecutive days to one of the following treatments: 0.5% of carboxymethyl cellulose (vehicle) suspension, administered orally (untreated, or UTG group); 50 mg kg^{-1} day^{-1} of Glucantime® (GLU), by intraperitoneal injection (GLU group); 50 mg kg^{-1} day^{-1} of ***imzt*** and 25 mg kg^{-1} day^{-1} of compound ***(4)***, administered orally as suspensions in 0.5% of carboxymethyl cellulose. After 10 days of treatment, animals were sacrificed in a CO_2 chamber, and a sample of the spleen and the liver (approximately 50 mg) was removed, weighed and used for total RNA extraction to subsequently undergo transformation into cDNA, as previously described [29].

DNA extraction

Standard curves of parasite DNA for use in quantitative real-time PCR (qPCR) experiments were produced as described previously [30]. In the log curve phase, the parasites were harvested, washed twice by centrifugation in phosphate-buffered saline (pH 7.2) at 1000 g for 10 min. A stock solution of 1×10^8 promastigotes of each strain was estimated by microscopic count and was used to prepare the standard curves. The parasite pellets were used to DNA extraction and determined the DNA concentration. Next, eight different concentrations of promastigotes were performed to obtain the points of the standard curve ranging from 1×10^7 to 1 promastigotes. DNA was extracted from samples using the QIAamp DNA extraction Mini Kit (Qiagen), according to the manufacturer's instructions.

RNA extraction and cDNA synthesis

Fragments of liver and spleen (~50 mg; weighed using sterile and disposable surgical material) removed from treated animals were placed in sterile microfuge tubes and frozen immediately at − 80 °C in storage buffer (RNAlater). RNA extraction was performed 24 h after fragment removal, using the RNeasy Mini Kit (Qiagen), according to the manufacturer's instructions. RNA samples were frozen immediately after extraction. For reverse-transcription into cDNA, 1 µL of dNTPs mix (10 mM) and 1 µL of random primers (3 µg μL^{-1}) were added to 11 µL of RNA sample, and samples were incubated in a thermal cycler for approximately 5 min, at 65 °C. Then, tubes were placed on ice for 20 s, and 2 µL of DTT (100 mM) and 4 µL 5× buffer (Tris–HCl 250 mM, pH 8.3, containing 375 mM KCl, 15 mM $MgCl_2$) were added, and samples were incubated again in the thermal cycler for 20 s, at 37 °C. Finally, 1 µL (200 U μL^{-1}) M-MLV RT enzyme was added and samples were incubated for 50 min, for cDNA synthesis. The purity of the cDNA sample was confirmed by

measuring the absorbance at 260/280 in a NanoDrop ND2000, and sample integrity was verified by agarose gel electrophoresis and PCR. Samples were frozen at − 20 °C for subsequent use in qPCR.

Parasite load estimation by LINJ31 quantitative PCR (qPCR)

Quantitative real time PCR (qPCR) was performed using the TaqMan® probe 5′CCT CCT TGG ACT TTG C3′ (double-labelled with FAM at the 5′-end and a non-fluorescent quencher at the 3′-end), and the primers LINJ31F (5′CCG CGT GCC TGT CG3′) and LINJ31R (5′CCC ACA CAA GGA GCG ACT3′), which amplify *L.* (*L.*) infantum *chagasi* hypothetical protein [31]. Reactions were performed in a 7500 Real Time PCR System (Applied Biosystems), and reaction mixtures contained 3 µL of DNA or cDNA samples (or control samples, see below), 10 µL of 2X TaqMan Universal PCR Master Mix, 1 µL of a mixture of forward (LINJ31F) and reverse (LINJ31R) primers (at a concentration of 18 µM), and 5 µM of the labelled TaqMan®probe, in a final volume of 20 µL. For negative and positive controls, water or DNA extract from *L.* (*L.*) *infantum chagasi* (MHOM/BR/1972/BH46) were added, respectively. The following PCR conditions were used: one step of 50 °C for 2 min, followed by one step of 95 °C for 10 min, and 40 cycles of 95 °C for 15 s and 60 °C for 1 min. The number of parasites per gram of spleen or liver tissue was calculated based on the linear regression data from the standard curve performed with promastigote DNA [29]. Statistical analysis was performed by Student's *t* test with Mann–Whitney (unpaired, two tailed) for the significance test ($p < 0.05$) [30].

Histopathological evaluation of non-infected hamsters

For histological analysis, fragments from liver and kidney collected from non-infected hamsters were fixed in 10% buffered formalin and processed through conventional histological techniques. Sections of 5 µm thick were stained with hematoxylin and eosin (HE) and analysed by a pathologist blinded to the experimental groups. Particular attention was paid to microscopic findings in liver such as steatosis, hydropic degeneration, necrosis, microabscesses, fibrosis and disorganization of hepatic cords; glomerular and tubular degeneration as well necrosis and fibrosis in kidney [32]. All sections were analysed under an optical light microscope (Zeizz Axio Scope A1) equipped with a camera (Axio Cam CC3, Zeizz).

Biological effects on *Leishmania*

Antiproteolytic activity

Inhibitory activity against rCPB 2.8 The procedure was performed using 1 mL of 100 mmol L^{-1} sodium acetate buffer (pH 5.5, containing 5 mmol L^{-1} EDTA, 100 mmol L^{-1} NaCl, 20% glycerol and 0.01% triton X-100), to which 3 mmol L^{-1} dithiothreitol (DTT) and enzyme were added. The mixture was left to pre-activate for 10 min, then the fluorogenic substrate Z-FR MCA (7.4 µmol L^{-1}) was added. The enzymatic activity was monitored by substrate hydrolysis at 360 nm excitation and 480 nm emission wavelengths in a spectrofluorimeter. The reaction solution was continuously stirred and the temperature maintained at 37 °C in thermostatically-controlled water bath. The values of the enzymatic activity were calculated by linear regression and expressed as UAF min^{-1} (arbitrary units of fluorescence per minute). The assays were repeated with two different concentrations (10 and 100 µmol L^{-1}) of each compound, enabling the activity values in UAF min^{-1} to be determined for each one. The values obtained in the absence of the compound were assumed to represent 100% activity, and the activity values in the presence of the compounds were calculated as a proportion of these values. Enzyme inhibition was expressed as the compound concentration causing a 50% decrease in enzyme activity (IC_{50} value) [11]. IC_{50} value was calculated by non-linear regression, based on dose–response curves using ***(1)***, ***(2)***, ***(3)***, ***(4)*** and ***Imzt*** compound at different concentrations, and the data were analysed with Grafit 5.0 software20 using Eq. (2):

$$y = \left(\frac{\text{Range}}{1 + \frac{x}{\text{IC50}}} \right). \tag{2}$$

In Eq. (2), y is the enzyme activity, x is the inhibitor concentration, and s is a slope factor. The equation assumes that y reduces with increasing x. As reference inhibitors were used E-64 for rCPB2.8 [11].

Determination of hydrogen peroxide release

Promastigotes (10^8 cells mL^{-1}) of *L.* (*L.*) *amazonensis* at lag (2 days) and log (4 days) phases of the proliferation curve treated or not (control) with compound ***(4)*** were incubated in reaction buffer 1X from Amplex Red® kit in the presence of 5 mM succinate, 40 µM digitonin, 0.1 U mL^{-1} horseradish peroxidase and 25 µM Amplex Red (Molecular Probes®). The fluorescence was monitored at the excitation and emission wavelengths of 571 nm and 585 nm, respectively, at 96-well plate using a Varian Cary Eclipse Fluorescence Spectrophotometer. The quantitative correlation between the fluorescence and the H_2O_2 released by the cells was determined as previously described [26]. The experiments were carried out in triplicate and were repeated independently three times.

Results and Discussion

Chemistry

The new complexes [Ag(phen)$_2$(imzt)]X {X$^-$ = NO_3^- ***(1)***, $CF_3SO_3^-$ ***(2)***} were prepared in acetonitrile by reacting the appropriate AgX salt, 1,10-phenanthroline (phen) and imidazolidine-2-thione (imzt) in a 1:1:1 molar ratio, respectively. Aiming to investigate which ligands were important for activity, the *bis*-chelated complex [Ag(phen)$_2$]BF_4·H_2O ***(3)*** and the binuclear compound [Ag_2(imzt)$_6$](NO_3)$_2$ ***(4)*** [25]. The complexes were air and light stable solids. Elemental analysis data revealed that ***(1)*** and ***(2)*** have molar ratios Ag^+: phen: imzt: X$^-$ = 1:1:1:1 (X$^-$ = NO_3^- and $CF_3SO_3^-$) whereas ***(3)*** displayed a 1:2:1 stoichiometry for Ag^+: phen: BF_4^-. The molar conductivity values of ***(1–3)*** in DMSO were found between 30 and 46 Ω^{-1} cm^2 mol^{-1}, in agreement with their 1:1 electrolytic behaviour [33]. These findings suggested that these complexes have mononuclear structure in solution, as observed in similar compounds reported by us [23]. The ESI/MS spectra of complexes ***(1)*** and ***(2)*** showed the expected signals of the mononuclear [Ag(phen)(imzt)]$^+$ ion at *m*/*z* 389, together with the presence of the peak at *m*/*z* 287 assigned to the [Ag(phen)]$^+$ ion. The ESI/MS spectrum of ***(3)*** showed the typical signals of the fragments [Ag(phen)$_2$]$^+$ and [Ag(phen)(OH_2)]BF_4^+ at *m*/*z* 467 and 391, respectively. In these cases, the observed isotope patterns were in agreement with those calculated for the formulated ions. Compound [Ag_2(imzt)$_6$](NO_3)$_2$ ***(4)*** has been successfully synthesized as described by literature [25].

Spectroscopic evidence provided relevant information on the structures of compounds ***(1)*** and ***(2)***. The shift to lower frequency of the νC=S band from 516 cm^{-1} (free imzt) to 494 ***(1)***, 498 cm^{-1} ***(2)*** suggested the coordination of imzt via S atom [34]. In addition, the displacement to higher frequency of the νCN absorption from 1522 cm^{-1} (free imzt) to ca. 1533 cm^{-1} in complexes (***1–2***) also supported the *S*-coordination of imzt. The chelating coordination mode of phen is supported by the appearance of its typical bands in the IR spectra of ***(1–3)*** at ca. 1590, 1426, and 726 cm^{-1}. The presence of uncoordinated NO_3^-, $CF_3SO_3^-$ and BF_4^- ions in ***(1)***, ***(2)*** and ***(3)***, respectively, was also inferred on the basis of IR evidence, confirming their cationic character.

The ^{1}H NMR spectra of ***(1–2)*** in DMSO-d_6 showed only one set of signals for coordinated phen and imzt, which suggests the presence of a single species in solution. The coordinated phen has equivalent halves due to the appearance of the four signals assigned to the H_2/H_2', H_3/H_3', H_4/$H_4'$and H_5/H_5' nuclei. For example, the NMR spectrum of complex ***(2)*** displayed two double doublets at 9.14 and 8.76 ppm, which are shifted 0.03 and 0.26 to downfield, respectively, as compared to the free ligand. One multiplet at 8.02 ppm and one singlet at 8.18 ppm experienced a downfield shift of 0.23 and 0.18 ppm, respectively. The integration curves of the ^{1}H NMR signals of complexes ***(1)*** and ***(2)*** indicated a 1:1 molar ratio of phen: imzt, which is in agreement with the analytical results. The coordination of neutral imzt is supported by the presence of broad NH resonance at ca. 8.9 ppm in ***(1)*** and ***(2)***, being shifted 1.0 ppm to downfield related to free ligand. Upon coordination, the –CH_2– singlet changed from 3.49 (free imzt) to 3.72 ppm in ***(1)*** and ***(2)***. Such displacements are attributed to the delocalization of π-electrons between nitrogen atoms as a result the strengthening of the CN bond together with the weakening of the CS bond on complex formation [34]. For ***(3)***, only the set of signals for coordinated phen was observed. The ^{13}C{^{1}H} NMR spectra of ***(1)*** and ***(2)*** confirmed the *S*-coordination mode of imzt. The C=S resonance was displaced from 183.4 ppm (free imzt) to 179 ppm in these complexes, as a result of the formation of Ag–S bond together with the downfield shift of 1.2 ppm of the –CH_2– signal.

Taking into account that the results from elemental analysis, conductivity measurements, mass spectrometry and NMR spectroscopy, compounds ***(1)*** and ***(2)*** may exist in solution as mononuclear species, such as [Ag(phen)(imzt)]$^+$ or [Ag(phen)(imzt)(DMSO)]$^+$. For ***(3)***, the existence of the complex ion [Ag(phen)$_2$]$^+$ in solution was observed. Infrared, ^{1}H and ^{13}C NMR spectra and MS/ESI results for the silver (I) compounds ***(1–3)*** are available in the Supplementary Material.

Biology

The growth kinetics of the parasites were studied before assessing the in vitro activity of the test compounds to assess extension of the log-phase to ensure that drug efficacy assays were conducted during that period.

In vitro tests are important in biomonitoring studies in the search for active principles associated with the detected antileishmanial activity [35]. Thus, compounds with better antileishmanial activities and selectivity index (SI), ratio between CC_{50} (macrophages) e IC_{50} (amastigotes) were selected and these data suggest that alternative treatments may be effective in controlling the disease.

Therefore, all synthesized compounds were initially evaluated in vitro for their antileishmanial activities against promastigote and amastigote forms of *L.* (*L.*) *amazonensis* and *L.* (*L.*) *infantum chagasi*. To identify the selectivity of binding of compounds to the parasites with little or no effect on host cells, the cytotoxicity assay of the compounds in murine peritoneal macrophages was performed to determine CC_{50}. Thus, SI was also determined (Table 1).

The results showed a dose-dependent inhibition of growth after the incubation time (data not shown). The inhibitory effect of the compounds against the promastigote and amastigote forms showed some different responses. Although stage-specific activity has been reported previously for antileishmanial drugs, this variation in the sensitivity is difficult to interpret as it could be due to differences in the rate of division; or exposure of intracellular and extracellular stages to drugs; or biochemical targets; or drug metabolism [36]. In this work, two *Leishmania* species were assayed and the results reflect differences in the sensitivity of these parasites to the compounds tested. This fact is not surprising and previous in vitro studies have shown differences in sensitivity of *Leishmania* species in different classes of drugs [37, 38].

The process of differentiation of *Leishmania* forms throughout their life cycle has been extensively studied [39]. Significant changes in mRNA expression and translation rates [40] allow the parasites to adjust to the environmental differences according to the phase of the cycle by changing biochemical processes. For example, the transition could be accompanied by an increase in the enzyme activity rates involved with gluconeogenesis, making this path essential for the amastigote form [40]. In addition, Mondal et al., 2014 demonstrated differences regarding the mitochondrial bioenergetics between the amastigote and promastigote forms of *L. donovani* [41]. Biochemical changes such as those involved with post-translational modifications [42] occur at all stages of differentiation, and comparative analyses from transcriptomic and proteomic data throughout genomic time clearly indicate that the differentiation process is highly regulated and coordinated revised in [43]. In this sense, the involvement of different signaling pathways in differentiation is evident, as well as those prevalent in the amastigote and promastigote forms revised in [43]. All these data confirm that it is not appropriate to extrapolate activities obtained for one form of the parasite to the other. The modulation of cell-mediated response and the cellular and biochemical pathways of amastigotes differ considerably from those of promastigotes, suggesting that the chemotherapeutic potential of antileishmanial drugs depend on their action against amastigotes [11]. Given that the amastigote is the parasitic form responsible for disease, it should constitute the chemotherapeutic target in studies of new antileishmanial agents [44].

Among the compounds tested, compound ***(4)*** was the most potent against amastigote forms of *L.* (*L.*) *amazonensis* and *L.* (*L.*) *infantum chagasi*, with IC_{50} of 1.88 µM and 8.05 µM, respectively; it was also the compound that stood out against the others against promastigote forms. According to these results, the highest concentration tested showed a lower infection rate (data not shown), and the results were comparable to the reference drug in the treatment (Amphotericin B), that is its IC_{50} showed that its activity was comparable to that of the amphotericin B control drugs (IC_{50} = 1.30 µM, 4.00 µM, respectively), in most tests. In addition, this compound was found to be the least toxic to human macrophages, with a CC_{50} of 94.06 µM and more selective folds (SI = 50.00, 11.7, respectively) than the standard drug amphotericin B (CC_{50} = 27.05 µM, SI = 20.8, 6.7, respectively). Considering SI, expressed as the ratio of cytotoxicity (CC_{50}) and antileishmanial potency (IC_{50}), compound ***(4)*** exhibited the best biological profile. Although an SI greater than 10 is necessary to ensure the safety of a drug [45], the results for compound ***(4)*** are very important for the development of new anti-*leishmania* drugs. Analysing the cytotoxicity results, the different concentrations of the compounds used did not generate significant cytotoxic effects, in comparison with the control group (cells without

Table 1 Antileishmanial activity in vitro against promastigote and amastigote forms of *L.* (*L.*) *amazonensis* and *L.* (*L.*) *infantum chagasi*, cytotoxicity, selectivity index values, of compounds ***(1)***, ***(2)***, ***(3)***, ***(4)*** and ***Imzt*** compared to Amphotericin B

Compounds	Promastigotes IC^{a}_{50}, µM (SI)[d]		Amastigotes IC^{a}_{50}, µM (SI)[d]		Macrophages CC^{b}_{50}, µM
	L. (*L.*) *amazonensis*	*L.* (*L.*) *infantum chagasi*	*L.* (*L.*) *amazonensis*	*L.* (*L.*) *infantum chagasi*	
(1)	17.8 ± 0.1 (6.5)	3.22 ± 0.01 (36.0)	2.87 ± 0.001 (40.4)	18.15 ± 0.003 (6.4)	115.97 ± 0.002
(2)	61.10 ± 0.01 (2.8)	4.40 ± 0.12 (38.7)	10.92 ± 0.003 (15.5)	37.82 ± 0.006 (4.5)	170.2 ± 0.04
(3)	44.54 ± 0.003 (2.21)	4.46 ± 0.02 (22.1)	3.61 ± 0.001 (27.3)	30.16 ± 0.05 (3.3)	98.63 ± 0.01
(4)	4.67 ± 0.001* (20.1)	9.35 ± 0.002 (10.0)	1.88 ± 0.001* (50.0)	8.05 ± 0.002* (11.7)	94.06 ± 0.01
Imzt	75.60 ± 0.001 (21.4)	243.50 ± 0.012 (6.6)	371.08 ± 0.01 (4.3)	248.43 ± 0.02 (6.5)	1620.00 ± 0.15
Amphotericin B	5.10 ± 0.002* (5.3)	3.46 ± 0.02 (7.8)	1.30 ± 0.001* (20.8)	4.00 ± 0.003* (6.7)	27.05 ± 0.001

*Non-statistical difference ($p < 0.01$) by Tukey's test

[a]Concentration for decrease of 50% infected macrophages in treated vs. non-treated wells

[b]Cytotoxicity concentration for 50% macrophages

[c]Each IC_{50} value represents the mean ± standard deviation of triplicate determined by the software Bioestat 5.0

[d]Selectivity Index (SI) = ratio CC_{50}(Macrophages)/IC_{50}(Amastigotes)

treatment), showing that they were not toxic to murine peritoneal macrophages.

Research demonstrated that Ag nanoparticles can be generated by biological synthesis, where they showed a higher antileishmanial effect and lower toxicity in host cells [46, 47], resulting in inhibition of parasite proliferation. Cytotoxicity was not observed in the treated macrophages, and a reduction in the growth of promastigote and amastigote forms was observed when they were treated with compound ***(4)***. Current therapy against leishmaniasis based on Amphotericin B and Glucantime®, has a variety of side effects, in addition to high toxicity [48]. Thus, it is extremely important to search for new compounds that are more effective in the treatment of leishmaniasis and with low toxicity. As described above, we obtained excellent results for compounds containing silver in their structure, with potent antileishmanial activities in vitro, in addition to presenting low toxicities in macrophages, compared to the standard drug.

In this sense, we evaluated the antiparasitic effect of compounds ***(4)*** and ***Imzt*** on established infection hamsters (60 days post-inoculation with *L.* (*L.*) *infantum chagasi*) through quantification of live amastigotes of *L.* (*L.*) *infantum chagasi* in the tissues of the liver and spleen. Therefore, a quantitative detection of the marker LINJ31 was used [29] (Fig. 1).

The results showed that the compound ***(4)*** reduced the number of amastigotes in the liver and spleen when compared to the untreated group (UTG). In addition, when comparing the effect of compound ***(4)*** and Glucantime® on the spleen, no significant difference was observed. In making a correlation between the compounds in question, we can conclude that the insertion of silver and nitrate into the chemical structure improved its activity in both, in vitro and in vivo assays. According to the literature, studies have shown that the addition of the nitrate group in metallic compounds may contribute to increase the antileishmanial activities in vitro in different evolutionary forms of *L.* (*L.*) *amazonensis* [49, 50].

Additionally, different routes of administration can lead to different pharmacological responses, due to variations in the absorption processes, since the absorbed dose is different from that administered [29]. The chemical nature of compounds can lead to different routes of absorption; as an example, compounds in solution can be absorbed faster than those in suspension [51]. This difference in the route of administration may have contributed to the increased efficacy of Glucantime®, also in the liver.

The liver from hamsters daily treated with 25 mg kg^{-1} day^{-1} of compound ***(4)*** exhibited some histological alterations in areas adjacent to centrilobular vein including disorganization of the hepatic cords, hydropic degeneration and necrotic cells with karyolytic or picnotic nuclei

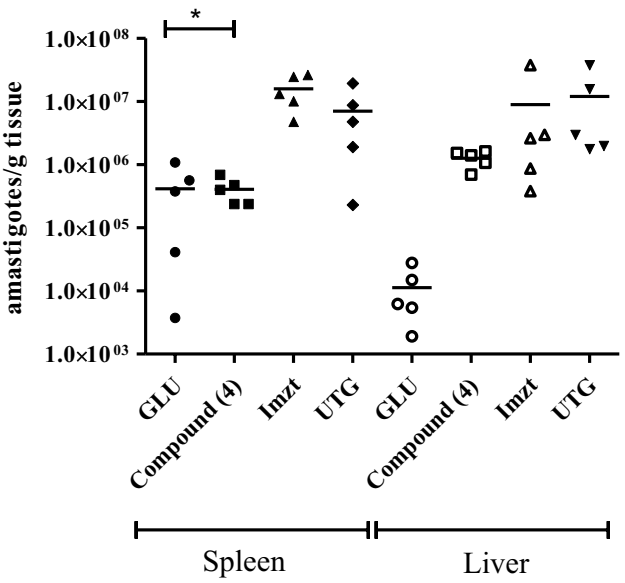

Fig. 1 Quantification of parasite burden in the spleen and liver from hamsters infected with *Leishmania* (*L.*) *infantum chagasi*, as quantified by PCR for the detection of the LINJ31marker. The numbers of parasites (amastigotes) per gram of tissue were estimated based on a qPCR standard curve using promastigotes. ***UTG***: untreated group (vehicle-treated), ***GLU***: animals treated with Glucantime® (50 mg/kg/day); ***Imzt***: compound imidazolidine-2-thione (50 mg/Kg/day); compound ***(4)*** (25 mg/kg/day). $n = 5$ animals/group. Data are represented as group mean and individual values for each animal. *Statistically similar ($p < 0.05$)

(Fig. 2a, b). Histological examination of kidney after compound ***(4)*** treatment revealed degenerative changes in some parenchymatous elements in comparison with untreated control. Atrophy of renal corpuscle and, degeneration and atrophy of lining epithelium in some renal tubules were occasionally noticed in some areas (Fig. 2c, d). However, no sign of significant histological changes such as microabscesses, fibrosis or marked loss of hepatic and/or renal tissue that would indicate a major toxicity were noticed after compound ***(4)***-treatment.

Biological effects on *Leishmania*

Since the effect of compound ***(4)*** on different forms of *Leishmania* has been observed, this fact led us to investigate which changes could be detected in the parasites incubated with the compound in question. Besides the fact that some compounds derived from imidazole exhibited activity of scavengers from reactive oxygen species [52]; and activity in proteases [53]. In this sense, since the compound ***(4)*** used in our experiments is an imidazole derivative, the evaluation of H_2O_2 production could be interesting, as well as the protease activity to be evaluated.

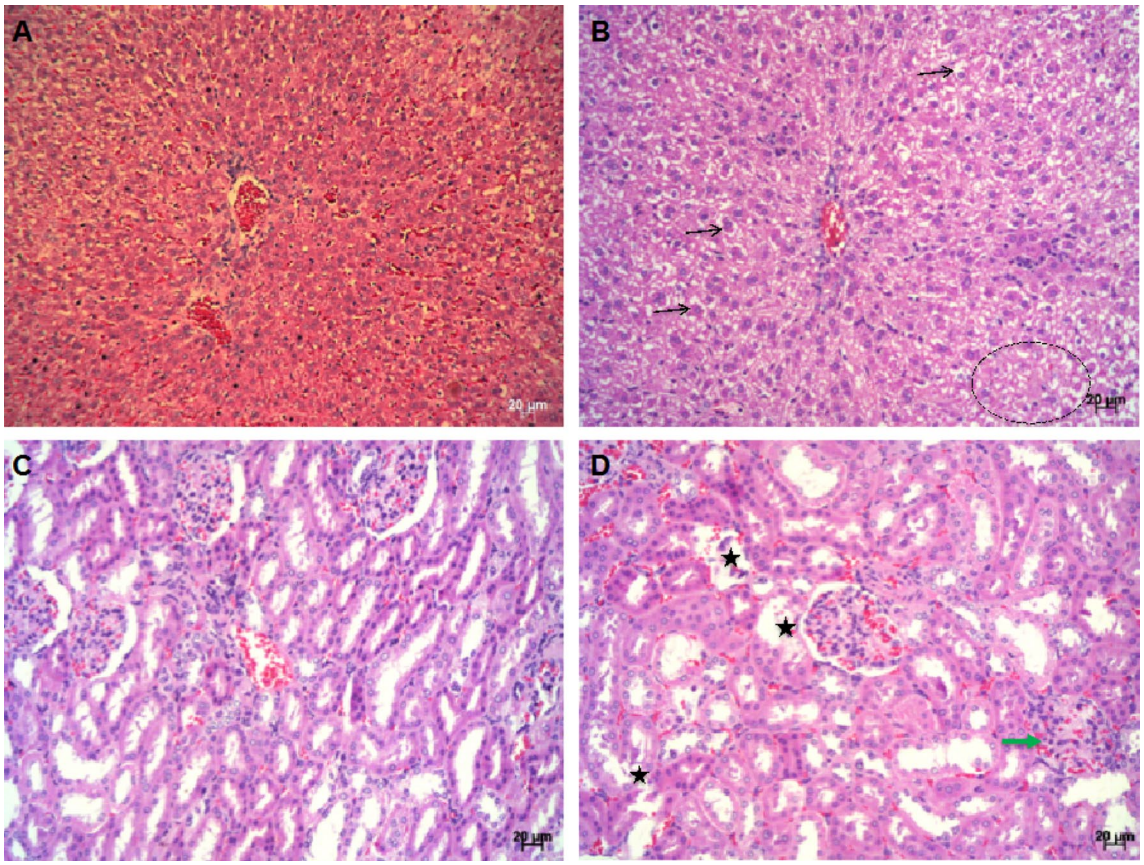

Fig. 2 Histological examination of non-infected hamsters liver and kidney after compound ***(4)*** treatment. Photomicrographs of livers after intraperitoneal administration of compound ***(4)*** at **a** untreated and **b** 25 mg/kg/day, respectively. Liver of hamsters daily injected with 25 mg/kg/day of compound ***(4)*** shows disorganization of hepatic cords at proximity to centrilobular vein, hydropic degeneration (arrows), and necrotic cells (circle). Sections of untreated (**c**) and compound ***(4)***-treated (**d**) hamsters kidneys, respectively. Kidney of compound ***(4)***-daily treated hamsters shows atrophy of renal corpuscle (green arrow), and degeneration and atrophy of some renal tubules (star). Original magnification ×200 (scale bar: 20 µm)

All compounds and the reference protease inhibitor E64 (trans-epoxysuccinyl-L-leucylamido(4-guanidino)butane) were next assayed to determine their inhibitory potential against cysteine proteases rCPB2.8 (Table 2).

The *L* (*L.*) *mexicana* assays are performed for not yet obtaining cysteine proteases from other *Leishmania* species. Therefore, by homology experiments in *L.* (*L.*) *mexicana* are accepted and used to infer the potential/activity against the cysteine proteases [11]. As can be seen, not all compounds presented as potent cysteine protease inhibitors B. The compound ***(1)*** was the most potent inhibitor compound against rCPB2.8 with IC_{50} value of 2.37 µM, but no less active than the E64 standard. Proteases are also key enzymes in the metabolism of proteins, or biologically active peptides [54]. These enzymes are also involved in several adaptation mechanisms for the survival of parasites: regulation of immune response, invasion and damage tissue, differentiation and dissemination of parasite and uptake of essential nutrients to parasite [54, 55]. In our experiments it was possible to observe that, although the compounds tested not present potent activity against the cysteine protease (CPB 2.8), when compared to the E64 standard, it was possible to speculate that this would not be the main mechanism of action presented by these compounds.

Table 2 Quantitative in vitro inhibitory effect of synthetic compounds on cysteine protease rCPB2.8 activity of *L.* (*L*) *mexicana,* compared to E64

Compounds	r-CPB2.8[a] IC50 (µM)
(1)	2.37 + 0.09
(2)	2.92 + 0.16
(3)	4.74 + 0.34
(4)	4.29 ± 0.08
Imzt	3.09 ± 0.08
E64	0.125 ± 0.006

[a] Each IC_{50} value represents the mean ± standard deviation of triplicate determined by the software Grafit 5.0

Thus, another possibility for the mechanism of action could be related to concentration of reactive oxygen species in the parasite. Therefore, we evaluated the production of hydrogen peroxide in *Leishmania* promastigotes treated with compound ***(4)***.

Leishmania, like other trypanosomatids, possesses a unique mitochondrion with peculiar characteristics, such as the presence of enzymes of exclusive metabolic pathways and a specific arrangement of mitochondrial DNA. During the life cycle of trypanosomatids, their unique mitochondria undergo profound changes, reflecting the adaptation to different environments, such as hypoxia and oxidative stress [55]. In parallel, the mitochondria are involved in the processes of differentiation, proliferation, calcium homeostasis, redox balance, and programmed cell death [56], beside being the main source of reactive oxygen species, such as hydrogen peroxide [57], but not the only one; since Machado et al. (2018) reported that *Leishmania* species are seen to make ROS through NADPH oxidase enzymes [58]. In this sense, the maintenance of mitochondrial integrity is fundamental for the survival of the parasite, therefore this organelle is a potential target in the development of drugs. The mechanism of action of some drugs, or even of potential drug candidates, involves pathways related to mitochondrial bioenergetics and generation of ROS.

For the survival of *Leishmania*, as well as other trypanosomatids, maintaining a reduced intracellular environment is necessary. This maintenance is done by the activity of antioxidant enzymes, such as peroxidases [59, 60]. In this sense, the increase in the production of H_2O_2 signals an increase in the synthesis of these antioxidant enzymes (cytosolic and mitochondrial enzymes) as previously reported [26], which guarantees a reduced intracellular environment and consequently the survival of the parasite [61], thereby avoiding oxidative stress. On the other hand, it was observed that the proliferation of parasites, as an example, *Trypanasoma cruzi*, also a trypanosomatid such as *Leishmania*; has a relation in terms of signaling with the concentration of H_2O_2 [62]. Low concentrations of H_2O_2 stimulate cell proliferation in *T. cruzi* [62], in mammalian [63] and yeast cells [64].

In recent years, the understanding of the importance of ROS as a regulator of biological and physiological response has increased [65–67], highlighting superoxide and hydrogen peroxide (H_2O_2) as co-products of mitochondrial respiration. Regarding H_2O_2, studies have shown that low levels of this reactive species are implicated in a reduction in growth and cell proliferation [68, 69], while high levels may lead to oxidative stress, leading to cell impairment. Researchers observed in *T. cruzi*, that in low concentrations of H_2O_2, cell proliferation was stimulated and parasites increased their resistance to sublethal doses of H_2O_2 (100 µM) if previously treated with a non-toxic H_2O_2 concentration (20 µM) [69].

Thus, to evaluate whether incubation with compound ***(4)*** could or could not lead to increased or decreased H_2O_2 production, we determined the H_2O_2 release in promastigotes *L.* (*L.*) *amazonensis* at lag and log phases of the proliferation curve treated with or without compound ***(4)***. In this experiment, using Amplex® red as a probe, under our experimental conditions, it was possible to notice that the level of peroxide production was maintained between the lag and log phases; however, after treatment with compound ***(4)*** there was a reduction of 25.44 and 49.13% in the peroxide rates when compared to the lag and log phases, respectively (Fig. 3). This result suggests this compound has a higher effect of reducing peroxide production in the log phase.

Additionally, Finzi et al. (2004) observed that the treatment of parasites with concentrations of 20 uM H_2O_2 signaled the increase in the number of parasites. In this sense, as observed in our results, the treatment with compound ***(4)*** led to a reduction in H_2O_2 production, and as previously observed [62]. The reduction of this reactive oxygen species reduces the signaling for cellular proliferation, which can be observed by the reduction in the number of parasites after treatment with the compound ***(4)***.

Thus, our results demonstrated the production of silver compounds and their greater effectiveness against the parasite *Leishmania*, highlighting a promising approach to improve drug efficacy in treatment of the disease. In addition, this study also demonstrated the reduction of toxicity, which is a major problem of the drugs currently used in treatment. Consistent with these findings and based on the

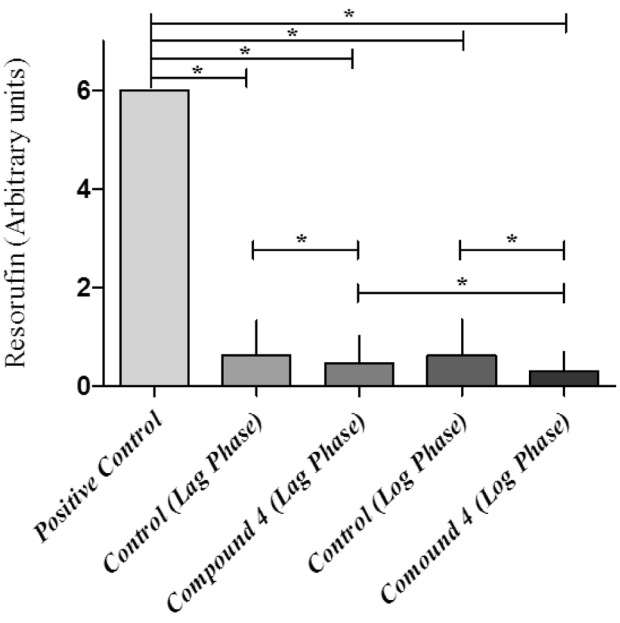

Fig. 3 Determination of H_2O_2 release in promastigotes *L.* (*L.*) *amazonensis* at lag and log phases of the proliferation curve treated or not with compound ***(4)***. *Present statistical difference

results obtained in our study; the silver and nitrate-containing compound is promising for the control of leishmaniasis and may represent an important option in the development of new drugs for the treatment of the disease.

Conclusion

In short, all compounds were evaluated for their antileishmanial and cytotoxicity properties. The most notable result was observed for compound ***(4)*** as the most active. In a comparative analysis of all the results, we verified that the modifications made in the molecule improved its activity in vitro and in vivo. Therefore, we conclude that probably the presence of a nitrate ion and the absence of the 1,10-phenanthroline ligand in the structure of the compound ***(4),*** together with its higher content of Ag^+ ions were important for the modulation of the antileishmanial activity. This compound may represent a promising model for the development of a new class of antileishmanial agents and deserves further investigation of its effects on *Leishmania* to obtain possible mechanisms of action.

Acknowledgements This work was sponsored by Grants from CNPq (proc. 487092/2012-0, INCT-INOFAR), FAPESP (2016/17711-5), CAPES and FAPEMIG.

References

1. Vijayakumar S, Pradeep DAS (2018) Recent progress in drug targets and inhibitors towards combting leishmaniasis. Acta Trop 181:95–104
2. World Health Organization (2016) Leishmaniasis, Geneva, p 375. http://who.int/mediacentre/factsheets/fs375/en/. Accessed Dec 2018
3. Akhoundi M, Downing T, Votýpka J, Kuhls K, Luke SJ, Cannet A, Ravel C, Marty P, Delaunay P, Kasbari M, Granouillac B, Gradoni L, Sereno D (2017) *Leishmania* infections: molecular targets and diagnosis. Mol Asp Med 57:1–29
4. Ghorbani M, Farhoudi R (2018) Leishmaniasis in humans: drug or vaccine therapy? Drug Des Dev Ther 12:25–40
5. World Health Organization (2018) WHO, Leishmaniasis. Geneva. http://who.int/leishmaniasis/clinical_forms_leishmaniases/en/index2.html. Accessed Dec 2018
6. Martínez DY, Verdonck K, Kaye PM, Adaui V, Polman K, Llanos-Cuentas A et al (2018) Tegumentary leishmaniasis and coinfections other than HIV. PLoS Negl Trop Dis 12(3):e0006125
7. Awasthi A, Mathur RK, Saha B (2004) Immune response to *Leishmania* infection. Indian J Med Res 119:238–258
8. Codonho BS et al (2016) HSP70 of *Leishmania amazonensis* alters resistance to different stresses and mitochondrial bioenergetics. Memórias do Instituto Oswaldo Cruz Rio de Janeiro 111(7):460–468
9. Savoia D (2015) Recent updates and perspectives on leishmaniasis. J Infect Dev Ctries 9(6):588–596
10. Oliveira LF, Schubach AO, Martins MM, Passos SL, Oliveira RV, Marzochi MC et al (2011) Systematic review of the adverse effects of cutaneous leishmaniasis treatment in the New World. Acta Trop 118(2):87–96
11. Gontijo VS, Espuri PF, Alves RB, Camargos LF, Santos FV, Judice WAS, Marques MJ, Freitas RP (2015) Leishmanicidal, antiproteolytic, and mutagenic evaluation of alkyltriazoles and alkylphosphocholines. Eur J Med Chem 101:24–33
12. Castro RAO, Silva-Barcellos NM, Licio CSA, Souza JB, Souza-Testasicca MC, Ferreira FM, Batista MA, Silveira-Lemos D, Moura SL, Frezard F, Rezende SA (2014) Association of liposome-encapsulated trivalent antimonial with ascorbic acid: an effective and safe strategy in the treatment of experimental visceral Leishmaniasis. PLoS One 9(8):104055
13. Shahverdi AR, Fakhimi A, Shahverdi HR, Minaian S (2007) Synthesis and effect of silver nanoparticles on the antibacterial activity of different antibiotics against *Staphylococcus aureus* and *Escherichia coli*. Nanomedicine. 3(2):168–171
14. Sarkar B, Kumar M, Verma S, Rathore RM (2015) Effect of dietary nanosilver on gut proteases and general performance in Zebrafish (Danio rerio). Int J Aquat Biol 3(2):60–67
15. Beck I, Hotowy A, Sawosz E, Grodzik M, Wierzbicki M, Kutwin M, Jaworski S, Chwalibog A (2015) Effect of silver nanoparticles and hydroxyproline, administered in ovo, on the development of blood vessels and cartilage collagen structure in chicken embryos. Arch Anim Nutr 69:57–68
16. Samuel U, Guggenbichler JP (2004) Prevention of catheter-rel the potential of a new nano silver impregnated catheter. Int J Antimicrob Agents 23S1:S75–S78
17. Asharani P, Sethu S, Lim HK, Balaji G, Valiyaveettil S, Hande MP (2012) Differential regulation of intracellular factors mediating cell cycle, DNA repair and inflammation following exposure to silver nanoparticles in human cells. Genome Integr 3(1):2–14
18. Yang EJ, Kim S, Kim JS, Choi IH (2018) Inflammasome formation and IL-1β release by human blood monocytes in response to silver nanoparticles. Biomaterials 33(28):6858–6867
19. Kumar N, Krishnani KK, Gupta SK, Singh NP (2018) Effects of silver nanoparticles on stress biomarkers of *Channa striatus*: immuno-protective or toxic? Environ Sci Pollut Res Int 25(15):14813–14826
20. Medici S, Peana M, Crisponi G, Nurchi VM, Lachowicz JI, Remelli M et al (2016) Silver coordination compounds: a new horizon in medicine. Coord Chem Rev 327–328:349–359
21. Mccann M, Geraghty M, Devereux M, O'shea D, Mason J, O'sullivan L (2000) Insights into the mode of action of the anticandida activity of 1,10-phenanthroline and its metal chelates. Metal Based Drugs 7(4):185–193
22. Navarro M, Cisneros-Fajardo EJ, Marchan C (2006) New silver polypyridyl complexes: synthesis, characterization and biologic activity on Leishmania mexicana. Arzneimittelforschung 56:600–604
23. Segura DF, Netto AVG, Frem RCG, Mauro AE, Da Silva PB, Fernandes JA, Almeida Paz FA, Dias ALT, Silva NC, De Almeida ET, Marques MJ, De Almeida L, Alves KF, Pavan FR, De Souza PC, De Barros HB, Leite CQF (2014) Synthesis and biological evaluation of ternary silver compounds bearingN,N-chelating ligands and thiourea: X-ray structure of $[\{Ag(bpy)(\mu\text{-}tu)\}_2](NO_3)_2$ (bpy=2,2′-bipyridine; tu=thiourea). Polyhedron 79:197–206
24. Cesarini S, Spallarossa A, Ranise A, Schenone S, Rosano C, la Colla P, Sanna G, Busonera B, Loddo R (2009) *N*-Acylated and *N*, *N*′-diacylated imidazolidine-2-thione derivatives and *N*, *N*′-diacylated tetrahydropyrimidine-2(1*H*)-thione analogues: synthesis and antiproliferative activity. Eur J Med Chem 44:1106–1118
25. Bowmaker GA, Chaichit N, Pakawatchai C, Skelton BW, AH A (2009) White, Structural and spectroscopic studies of some adducts of silver(I) salts with ethylenethiourea. Can J Chem 87:161–170

26. Peloso EF, Gonçalves CC, Silva TM, Ribeiro LH, Piñeyro MD, Robello C, Gadelha FR (2012) Tryparedoxin peroxidases and superoxide dismutases expression as well as ROS release are related to *Trypanosoma cruzi* epimastigotes growth phases. Arch Biochem Biophys 15(520–2):117–122
27. Arrais-Silva WW, Colhone MC, Ayres DC, Souto PCS, Giorgio S (2005) Effects of hyperbaric oxygen on *Leishmania amazonensis* promastigotes and amastigotes. Parasitol Int 54(1):1–7
28. Mosmann T (1983) Rapid colorimetric assay for cellular growth and survival: application to proliferation and cytotoxic assays. J Immunol Methods 65:55–63
29. Colombo FA, Reis RA, Nunes JB, Dias DF, Dos Santos MH et al (2017) In vivo evaluation of leishmanicidal activity of benzophenone derivatives by qPCR. Med Chem (Los Angeles) 7:890–893
30. Colombo FA, Pereira-Chioccola VL, Da Silva Meira C, Motoie G, Gava R et al (2015) Performance of a real time PCR for leishmaniasis diagnosis using a *L.* (*L.*) *infantum* hypothetical protein as target in canine samples. Exp Parasitol 157:156–162
31. Colombo FA et al (2011) Detection of *Leishmania* (*Leishmania*) *infantum* RNA in fleas and ticks collected from naturally infected dogs. Parasitol Res 109(2):267–274
32. Gutiérrez-Rebolledo GA, Siordia-Reyes AG, Meckes-Fischer M, Jiménez-Arellanes A (2016) Hepatoprotective properties of oleanolic and ursolic acids in antitubercular drug-induced liver damage. Asian Pac J Trop Med 9(7):644–651
33. Geary WJ (1970) The use of conductivity measurements in organic solvents for the characterisation of coordination compounds. Coord Chem Rev 7:81–122
34. De Moura TR, Cavalcanti SL, Godoy PRDV, Hojo ETS, Rocha FV, De Almeida ET, Deflon VM, Mauro AE, Netto AVG (2017) Synthesis, characterization and antitumor activity of palladium(II) complexes of imidazolidine-2-thione. Transit Met Chem 42:565–574
35. Bezerra LJ et al (2006) Avaliação da atividade leishmanicida *in vitro* de plantas medicinais. Revista Brasileira de Farmacognosia 16:631–637
36. Escobar P et al (2002) Sensitivities of *Leishmania* species to hexadecylphosphocholine (miltefosine), ET-18-OCH3 (edelfosine) and amphotericin B. Acta Trop 81:151–157
37. Morais-Teixeira E, Carvalho AS, Costa JCS, Duarte SL, Mendonça JS, Boechat N, Rabello A (2008) In vitro and in vivo activity of meglumine antimoniate produced at Farmanguinhos-Fiocruz, Brazil, against *Leishmania* (*Leishmania*) *amazonensis, L* (*L.*) *chagasi* and L (*Viannia*) *braziliensis*. Mem Inst Oswaldo Cruz 103:358–362
38. De Carvalho GSG, Machado PA, De Paula DTS, Coimbra ES, Da Silva AD (2010) Synthesis, cytotoxicity, and antileishmanial activity of *N*, *N*′-disubstituted ethylenediamine and imidazolidine derivatives. Sci World J 10:1723–1730. https://doi.org/10.1100/tsw.2010.176
39. Barak E, Amin-Spector S, Gerliak E, Goyard S, Holland N, Zilberstein D (2005) Differentiation of *Leishmania donovani* in host-free system: analysis of signal perception and response. Mol Biochem Parasitol 141:99–108
40. Mottram JC, Coombs GH (1985) *Leishmania* mexicana: enzyme activities of amastigotes and promastigotes and their inhibition by antimonials and arsenicals. Exp Parasitol 59:151–160
41. Mondal S, Roy JJ, Berat T (2014) Characterization of mitochondrial bioenergetic functions between two forms of *Leishmania donovani*—a comparative analysis. J Bioenerg Biomembr 46(5):395–402
42. Lahav T, Sivam D, Volpin H, Ronen M, Tsigankov P, Green A, Holland N, Kuzyk M, Borchers C, Zilberstein D, Myler PJ (2011) Multiple levels of gene regulation mediate differentiation of the intracellular pathogen *Leishmania*. FASEB J 25:515–525
43. Kima PE (2007) The amastigote forms of *Leishmania* are experts at exploiting host cell processes to establish infection and persist. Int J Parasitol 37(10):1087–1096
44. Robledo S, Osorio E, Munõz D, Jaramillo LM, Restrepo A, Arango G, Vélez I (2005) In vitro and in vivo cytotoxicities and antileishmanial activities of thymol and hemisynthetic derivatives. Antimicrob Agents Chemother 49(4):1652–1655
45. Pires CM, Rodrigues SD, Bristot D, Gaeta HH, Toyama DO, Farias WRL, Toyama MH (2013) Evaluation of macroalgae sulfated polysaccharides on the *Leishmania* (*L.*) *amazonensis* promastigote. Mar Drugs 11:934–943
46. Gelvez APC, Farias LH, Pereira VS et al (2018) Biosynthesis, characterization and leishmanicidal activity of a biocomposite containing AgNPs-PVP-glucantime. Nanomedicine (Lond) 13(4):373–390
47. Ovais M, Khalil T, Raza A et al (2016) Green synthesis of silver nanoparticles via plant extracts: beginning a new era in cancer theranostics. Nanomedicine 11(23):3157–3177
48. Mendonça DVC et al (2018) Comparing the therapeutic efficacy of different amphotericin B-carrying delivery systems against visceral leishmaniasis. Exp Parasitol 186:24–35
49. Andrade JM et al (2016) Silver and nitrate oppositely modulate antimony susceptibility through aquaglyceroporin in *Leishmania* (*Viannia*) species. Antimicrob Agents Chemother 60:4482–4489
50. Franco LP, Cicillini SA, Biazzotto JC, Schiavon A, Mikhailovsky A, Burks P, Garcia J, Ford PC, Da Silva RS (2014) Photoreactivity of a quantum dot-ruthenium nitrosyl conjugate. J Phys Chem A 118:12184–12191
51. Ning ZH, Long S, Zhou YY, Peng ZY, Sun YN et al (2015) Effect of exposure routes on the relationships of lethal toxicity to rats from oral, intravenous, intraperitoneal and intramuscular routes. Regul Toxicol Pharmacol 73:613–619
52. Berczyński P, Duchnik E, Kruk I, Piechowska T, Aboul-Enein HY, Bozdağ-Dündar O, Ceylan-Unlusoy M (2014) 6-Methyl 3-chromonyl 2,4-thiazolidinedione/2,4-imidazolidinedione/2-thioxo-imidazolidine-4-one compounds: novel scavengers of reactive oxygen species. Luminescence 29(4):367–373
53. Weng Z, Shao X, Graf D, Wang C, Klein C, Wang J, Zhou G-C (2016) Identification of the fused bicyclic derivatives of pyrrolidine and imidazolidinone as dengue virus-2 NS2B-NS3 protease inhibitors. Eur J Med Chem 125:751–759. https://doi.org/10.1016/j.ejmech.2016.09.063
54. Coombs GH, Mottram JC (1997) Parasite proteinases and amino acid metabolism: possibilities for chemotherapeutic exploitation. Parasitology 114(Suppl):S61–S80
55. Aparicio IM, Scharfstein J, Lima AP (2004) A new cruzipain-mediated pathway of human cell invasion by *Trypanosoma cruzi* requires trypomastigote membranes. Infect Immun 72:5892–5902
56. Duchen MR (2000) Mitochondria and calcium: from cell signaling to cell death. J Physiolol 529:57–68
57. Vercesi AE, Kowaltowski AJ, Oliveira HC, Castilho RF (2006) Mitochondrial Ca^{2+} transport, permeability transition and oxidative stress in cell death: implications in cardiotoxicity, neurodegeneration and dyslipidemias. Front Biosci 11:2554–2564
58. Machado N, Gomes D, Vieira L, Nascimento M, Mittra B, Andrews N (2018) A new source of reactive oxygen species in *Leishmania amazonensis*: characterization of a heme-activated NADPH oxidase-like. Free Radic Biol Med 128(Supplement 1):S55
59. Wilkinson SR, Temperton NJ, Mondragon A, Kelly JM (2000) Distinct mitochondrial and cytosolic enzymes mediate trypanothione-dependent peroxide metabolism in *Trypanosoma cruzi*. J Biol Chem 275(11):8220–8225
60. Piacenza L, Peluffo G, Alvarez MN, Kelly JM, Wilkinson SR, Radi R (2008) Peroxiredoxins play a major role in protecting

Trypanosoma cruzi against macrophage- and endogenously-derived peroxynitrite. Biochem J 410(2):359–368
61. Piacenza L, Zago MP, Peluffo G, Alvarez MN, Basombrio MA, Radi R (2009) Enzymes of the antioxidant network as novel determiners of *Trypanosoma cruzi* virulence. Int J Parasitol 39(13):1455–1464
62. Finzi JK, Chiavegatto CW, Corat KF, Lopez JA, Cabrera OG, Mielniczki-Pereira AA, Colli W, Alves MJ, Gadelha FR (2004) *Trypanosoma cruzi* response to the oxidative stress generated by hydrogen peroxide. Mol Biochem Parasitol 133(1):37–43
63. Wiese AG, Pacifici RE, Davies KJ (1995) Transient adaptation of oxidative stress in mammalian cells. Ach Biochem Biophys 318:231–240
64. Davies JMS, Lowry CV, Davies KJA (1995) Transient adaptation to oxidative stress in yeast. Arch Biochem Biophys 317:1–6
65. Sena LA, Chandel NS (2012) Physiological roles of mitochondrial reactive oxygen species. Mol Cell 48:158–167
66. Reczek CR, Chandel NS (2015) ROS-dependent signal transduction. Curr Opin Cell Biol 33:8–13
67. Schieber M, Chandel NS (2014) ROS function in redox signaling and oxidative stress. Curr Biol 24:R453–R462
68. Lennicke C, Rahn J, Lichtenfels R, Wessjohann LA, Seliger B (2015) Hydrogen peroxide–production, fate and role in redox signaling of tumor cells. Cell Commun Signal 13:39
69. Lee S, Tak E, Lee J, Rashid MA, Murphy MP, Ha J, Kim SS (2011) Mitochondrial H_2O_2 generated from electron transport chain complex I stimulates muscle differentiation. Cell Res 21:817–834

Affiliations

Patrícia Ferreira Espuri[1,5] · Larissa Luiza dos Reis[1] · Eduardo de Figueiredo Peloso[2] · Vanessa Silva Gontijo[3] · Fábio Antônio Colombo[1] · Juliana Barbosa Nunes[1] · Carine Ervolino de Oliveira[1] · Eduardo T. De Almeida[3] · Débora E. S. Silva[4] · Jessica Bortoletto[4] · Daniel Fonseca Segura[4] · Adelino V. G. Netto[4] · Marcos José Marques[1,5]

✉ Patrícia Ferreira Espuri
patyespuri@hotmail.com

✉ Marcos José Marques
marques.prppg@gmail.com

[1] Laboratory of Parasitology, Department of Pathology and Parasitology, Institute of Biomedical Sciences, Universidade Federal de Alfenas, Alfenas, Minas Gerais CEP 37130-001, Brazil

[2] Department of Biochemistry, Institute of Biomedical Sciences, Universidade Federal de Alfenas, Alfenas, Minas Gerais CEP 37130-000, Brazil

[3] Laboratory of Researche on Medicinal Chemistry, Institute of Chemistry, Universidade Federal de Alfenas, Alfenas, MG 37133-840, Brazil

[4] Institute of Chemistry, UNESP-Univ. Estadual Paulista, P.O. Box 355, Araraquara, São Paulo 14801-970, Brazil

[5] Institute of Biomedical Sciences, Federal University of Alfenas, 700 Gabriel Monteiro da Silva St, Alfenas, MG 37130-000, Brazil